Cadherin interaction probed by atomic force microscopy

W. Baumgartner*, P. Hinterdorfer†, W. Ness*, A. Raab†, D. Vestweber‡, H. Schindler†, and D. Drenckhahn*§

*Institute of Anatomy, University of Würzburg, Koellikerstrasse 6, D-97070 Würzburg, Germany; †Institute for Biophysics, University of Linz, A-4040 Linz, Austria; and ‡Institute of Cell Biology, University of Münster, D-48149 Münster, Germany

Communicated by Martin Lindauer, University of Würzburg, Würzburg, Germany, February 7, 2000 (received for review November 17, 1999)

Single molecule atomic force microscopy was used to characterize structure, binding strength (unbinding force), and binding kinetics of a classical cadherin, vascular endothelial (VE)-cadherin, secreted by transfected Chinese hamster ovary cells as cis-dimerized full-length external domain fused to Fc-portion of human IgG. In physiological buffer, the external domain of VE-cadherin dimers is a ≈20-nm-long rod-shaped molecule that collapses and dissociates into monomers (V-shaped structures) in the absence of Ca^{2+}. Trans-interaction of dimers is a low-affinity reaction ($K_D = 10^{-3}$–10^{-5} M, $k_{off} = 1.8\ s^{-1}$, $k_{on} = 10^3$–$10^5\ M^{-1}{\cdot}s^{-1}$) with relatively low unbinding force (35–55 pN at retrace velocities of 200–4,000 $nm{\cdot}s^{-1}$). Higher order unbinding forces, that increase with interaction time, indicate association of cadherins into complexes with cumulative binding strength. These observations favor a model by which the inherently weak unit binding strength and affinity of cadherin trans-interaction requires clustering and cytoskeletal immobilization for amplification. Binding is regulated by low-affinity Ca^{2+} binding sites ($K_D = 1.15$ mM) with high cooperativity (Hill coefficient of 5.04). Local changes of free extracellular Ca^{2+} in the narrow intercellular space may be of physiological importance to facilitate rapid remodeling of intercellular adhesion and communication.

cell adhesion | VE-cadherin | binding strength | binding kinetics

Adhesive contacts between neighboring cells play a crucial role in various aspects of tissue organization, differentiation, and function. The important biological and medical aspects of such stable intercellular adhesions are well established (1).

In cellular monolayers that form permeability barriers, such as the simple epithelial lining of the intestine or the vascular endothelium covering the inner surface of blood vessels, adhesion between cells is mainly accomplished by Ca^{2+}-dependent adhesion molecules named cadherins (1, 2). The predominant cadherin of most epithelia is E-cadherin, whereas endothelial cells adhere to each other by vascular endothelial-cadherin (VE-cadherin) (3). Cadherins are type I single membrane-spanning cell surface proteins that require free extracellular Ca^{2+} for homophilic interaction of their N-terminal extracellular domains with cadherins of adjoining cells (4).

The rod-shaped external domain of classical cadherins is composed of five tandemly repeated ≈110-aa-long subdomains. The outermost N-terminal subdomain (subdomain 1) including the linker region to subdomain 2 can associate laterally to form cis-interacting parallel dimers (5, 6). These cis-dimers are assumed to represent the functional units required for adhesive activity (7, 8). In this model, adhesive bonds between cadherins of interacting cell membranes are predicted to result from binding between subdomains 1 of oppositely oriented cis-dimers to form trans-interacting antiparallel tetramers that are termed adhesion dimers. The binding constants for adhesion dimer formation and the force transmitted by adhesion dimers are still unknown. X-ray crystallographic studies of subdomain 1 of N-cadherin suggest that adhesion dimers might associate laterally into zipper-like supramolecular clusters providing cumulative adhesive strength (5). Adhesion dimers and zipper-like associations were not observed in crystals of E-cadherin subdomains 1–2 (6, 9).

In the present study, we applied atomic force microscopy (AFM) (10) as a powerful molecular approach to probe specific trans-interaction forces and conformational changes of recombinant VE-cadherin strand dimers in aqueous physiological conditions (11–15). Elementary trans-interactions observed between strand dimers revealed Ca^{2+}-dependent highly specific molecular recognition properties that provide a basis for modeling cadherin-mediated intercellular adhesion.

Materials and Methods

Recombinant VE-Cadherin-Fc. A VE-cadherin-Fc fusion protein was generated by placing a cDNA fragment coding for the complete extracellular part of mouse VE-cadherin, including the membrane proximal glutamine, in front of a cDNA fragment coding for the Fc part of human IgG1, including the hinge region and Ig domains CH2 and CH3. Construction of the expression plasmid, cell transfection, and production of the fusion protein was done essentially as described (16). The secreted VE-cadherin-Fc chimera were purified from the culture supernatants of stably transfected Chinese hamster ovary (CHO) cells by affinity chromatography using protein A agarose. In SDS/10%PAGE under nonreducing conditions, purified VE-cadherin-Fc migrated as a single band at 160–180 kDa (Fig. 1*A*) that corresponds to the calculated molecular weight of the chimeric protein (176,000). In immunoblots, the 160–180 kDa band reacted with both monoclonal VE-cadherin antibody (16) and anti-human IgG (Dianova, Hamburg, Germany).

Single-Molecule Imaging. Purified VE-cadherin-Fc was adsorbed to freshly cleaved mica at 0.5 μg/ml in buffer A (5 mM Hepes, 150 mM NaCl, adjusted with NaOH to pH 7.4) containing either 5 mM $CaCl_2$ or 5 mM EGTA. For single-molecule imaging, dynamic force microscopy (17, 18) was carried out in buffer A in the absence or presence of Ca^{2+} using a Macmode PicoSPM magnetically driven AFM (Molecular Imaging, Phoenix, AZ) equipped with a commercial fluid cell and with a Molecular Imaging Macmode interface driving a Nanoscope IIIa controller (Digital Instruments, Santa Barbara, CA). Cantilevers (Maclevers; Molecular Imaging) had a spring constant of 0.1 $N{\cdot}m^{-1}$. Free tip oscillation amplitude was 5 nm at 5 kHz driving frequency. Feedback was adjusted to 20% amplitude reduction.

Force Measurements. Measurements were carried out in buffer A (various Ca^{2+} concentrations) using a Nanoscope IIIa AFM equipped with a commercial fluid cell (Digital Instruments).

Abbreviations: VE-cadherin, vascular endothelial cadherin; CHO, Chinese hamster ovary; AFM, atomic force microsopy; PEG, polyethylene glycol; v_r, retrace velocity.

§To whom reprint requests should be addressed. E-mail: anat015@mail.uni-wuerzburg.de.

The publication costs of this article were defrayed in part by page charge payment. This article must therefore be hereby marked "*advertisement*" in accordance with 18 U.S.C. §1734 solely to indicate this fact.

Article published online before print: *Proc. Natl. Acad. Sci. USA*, 10.1073/pnas.070052697. Article and publication date are at www.pnas.org/cgi/doi/10.1073/pnas.070052697

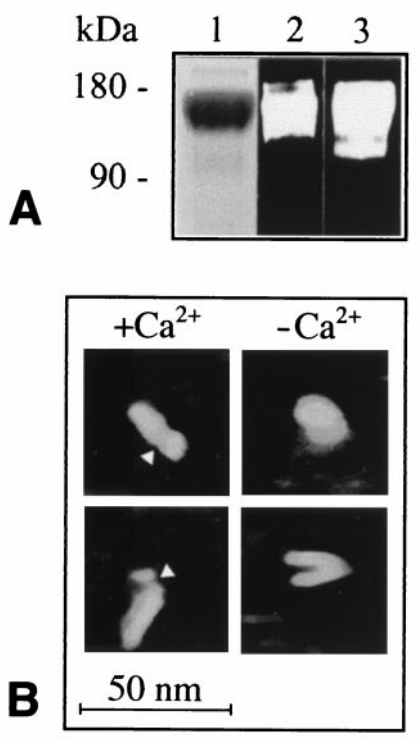

Fig. 1. Purified VE-cadherin-Fc characterized by SDS/PAGE and immunoblotting (*A*) and by AFM imaging (*B*). (*A*) SDS/PAGE was stained with Coomassie blue (1), and immunoblots were probed with VE-cadherin antibody (mAb 11D4.1) (2) and antibody against human IgG (3). Electrophoretic mobility (160–180 kDa) corresponds exactly to the calculated molecular weight of the chimeric dimer. (*B*) AFM images of hydrated VE-cadherin-Fc adsorbed to mica and scanned in the presence and absence of Ca^{2+} in isotonic buffer. Note elongated rod-like structure in Ca^{2+} and globular to v-shaped morphology in the absence of Ca^{2+}. Arrowheads point to constrictions assumed to mark the boundary between the Fc-portion and the cadherin moiety.

VE-cadherin-Fc was linked covalently to the Si_3N_4-tips of the cantilever (Park Scientific, Sunnyvale, CA) and SiOH plates (Wacker, Burghausen, Germany) using polyethylene glycol spacers (PEG 24) containing an amino-reactive crosslinker group (*N*-hydroxysuccinimide ester, NHS ester) at one end and a thiol-reactive group (2-[pyridyldithio]propionate, PDP) at the other end, as described in detail recently (19–21). The NHS group served to link PEG to free amino groups of both the Si_3N_4 tip and the SiOH plate introduced by treatment of tip and plate with 2-aminoethanol HCl (Sigma). The average labeling density of VE-cadherin-Fc (assayed by ELISA) (20) was calculated to be in the range of about 400–800 molecules/μm^2 surface.

Unbinding forces between tip-bound cadherin molecules (sensors) and plate-bound molecules (probe) were monitored by force-distance cycles at amplitudes of 100 and 200 nm, respectively, and at frequencies ranging from 1 to 10 Hz. Some experiments were carried out in which the tip was allowed to rest on the plate for up to 0.5 s before being retracted at velocities (v_r) ranging from 200 to 500 nm·s^{-1}. Force-distance cycles were performed either at constant lateral positions or with lateral shifts of 1 nm·s^{-1}. Spring constant of the cantilever (k_c) in force measurements was 0.03 ± 0.007 N·m^{-1} (determined by thermal noise analysis) (22). Force-distance cycles were analyzed as described in detail (23).

Results

Structure of VE-Cadherin-Fc. AFM imaging of hydrated VE-cadherin-Fc adsorbed to mica surface in buffer A containing 5 mM $CaCl_2$ revealed an elongated rod-like morphology (Fig. 1*B*) with a long axis of 25–28 nm and a short axis of 5–8 nm. Many molecules showed asymmetric constrictions separating them in a ≈20-nm rod-like portion (assumed to represent the cadherin moiety) and a shorter globular part ≈5–8 nm in diameter (probably representing the Fc-moiety). Molecules adsorbed and scanned in the absence of Ca^{2+} displayed globular or V-shaped morphologies with varying dimensions. Rod-shaped molecules were virtually absent under these conditions.

Force Measurements: General Considerations and Specificity. Recognition forces between homophilically binding VE-cadherin-Fc strand dimers attached to tip and plate of the AFM were determined by vertical approach-retrace cycles of the plate (Fig. 2*A*) (reviewed in ref. 20). During upward movement (approach), the plate eventually contacts the tip, and, as it moves further upwards, causes deflection of the cantilever that is proportional to the force. The uppermost position of the plate during the approach phase is defined as zero position of the force-distance curve. During down movement (retrace), the repulsive force of the upwards deflected cantilever causes the tip to follow the plate with the same linear force slope until the neutral position is reached at which the plate will separate from the tip if no attachment occurs. During the following phase of the retrace movement, the unattached cantilever remains unbent and stays at the neutral force position. If, however, the tip adheres to the plate, the cantilever will be pulled down below the neutral position until a critical force is reached at which the bond between the molecules attached to tip and plate breaks (unbinding force, f_u). The unbinding event is characterized by an abrupt jump of the force curve to the neutral position. In the present study, adhesion molecules were not directly attached to tip and plate but connected to the surface by a distensible PEG-linker. The force acting on the attached cantilever under these conditions will not follow a linear retrace force slope as one would see with direct (unspecific) plate-to-tip adhesion (Fig. 2*A*). Rather, the resulting force will follow a delayed nonlinear course reflecting the stretching of the flexible PEG-linker and the attached protein with increasing pulling force. The total tether length between tip and plate at which unbinding occurs is defined as unbinding length (l_u).

Adhesive Strength of Homophilic Trans-Interaction. Force-distance recordings of approach-retrace cycles at retrace velocity (v_r) of 800 nm·s^{-1} and total tip-to-plate contact time (encounter time) of 0.1 s showed specific recognition events (unbinding events) between tip- and plate-bound VE-cadherin-Fc (Fig. 2*B*). The number of unbinding events per cycle displayed local variations at different sites of the same plate, as expected from local variations of coupling density of plate-bound PEG/VE-cadherin-Fc. The unbinding forces ranged mainly between 15 and 150 pN. Depending on the individual signal-to-noise ratio of each unbinding event, values below 15 pN were mostly not significant. Fig. 2*B* shows examples of retraces with multiple unbinding events reflecting several independent recognition events during an individual cycle. In the case of multievent retraces, only the value of the last unbinding event of each force-distance cycle was measured (23). The absence of Ca^{2+} (EGTA) and the presence of VE-cadherin antibody caused complete inhibition of recognition events.

The distribution of unbinding forces of 500 successive unbinding events recorded at v_r = 800 nm·s^{-1} and tip-to-plate encounter duration of 0.1 s is plotted in Fig. 3*A* as a probability density function. Three distinct peaks are seen that closely match three overlapping Gaussian curves with maxima at 41, 75, and 120 pN, respectively. These data suggest multimeric cooperative interaction of the cadherins, with 40 pN being the adhesive strength quantum of a single adhesion dimer (v_r = 800 nm·s^{-1}). The observed

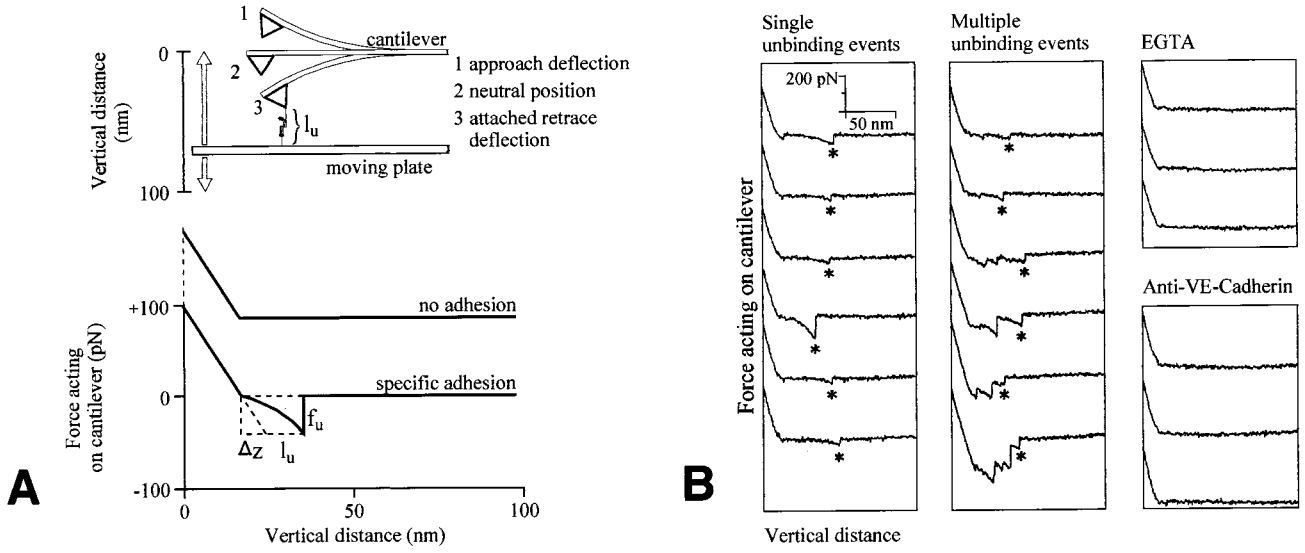

Fig. 2. General working principles of force measurements (*A*) and examples of force distance recordings (*B*). (*A*) Chimeric VE-cadherin-Fc is covalently attached by PEG linkers to plate and cantilever tip of the AFM. Cadherins bound to tip and plate by flexible PEG linkers are capable of free equilibrium diffusion and interaction with opposing cadherins during tip-to-plate encounter. Molecules are brought into binding contact by upward movement of the plate. During downmovement the force required for unbinding (f_u) is proportional to deflection to the cantilever (Δz) and its known spring constant. The total length of the stretched PEG-adhesion dimer is defined as unbinding length (l_u). (*B*) Force-distance curves obtained at a retrace velocity of 800 nm·s^{-1} and 0.1 s encounter duration in buffer A containing 2 mM Ca^{2+}. Examples of single unbinding events and multiple unbinding events are shown. Asterisks mark unbinding events taken for statistical evaluation. Unbinding events were completely abolished by addition of EGTA (5 mM) and antibody to VE-cadherin external domain.

multiples of the unitary unbinding force are considered to result from lateral association and load-induced "all-or-none" cooperative dissociation of three and more trans-interacting strand dimers (Fig. 3*B*). Simultaneous unbinding of two to three independent adhesion dimers would be an extremely unlikely process (see *Discussion*). Lateral oligomerization would be possible because of the high surface density of cadherin (mean distance estimated to be 30–40 nm) and of the ability of PEG-linked cadherins to undergo free diffusion and collision within a range determined by the length of the flexible PEG-linkers (extended lengths of 8–40 nm, unpublished observations).

To address the question whether association of cadherins into complexes with higher order unbinding strengths is a time-dependent process, we kept the retrace velocity constant, but allowed plate and tip to stay in contact for increasing periods (encounter duration). The results obtained by such an experimental series using the same tip at unchanged position on the plate (Fig. 3*B*) demonstrate that the probability of higher order unbinding forces increases with increasing encounter duration. At an encounter duration of 0.3 s, the 70–80 pN unbinding events occurred more frequently than the 40 pN units and at 0.5 s all three categories of binding, i.e., 40, 70–80, and 100–120 pN, occurred with a similar probability.

Dependence of Adhesive Strength and Lifetime of Bonds on Retrace Velocity. Stepwise increase of v_r from 200 to 4,000 nm·s^{-1} resulted in a logarithmic increase of the unbinding forces (Fig. 4). Only the unbinding forces of the first peak (single adhesion dimers) are included in Fig. 4, showing an increase of the mean from 33 pN at v_r = 200 nm·s^{-1} to 54 pN at v_r = 4,000 nm·s^{-1}.

Consistent with recent theoretical considerations (24, 25) and experimental data (26), these findings show that unbinding forces have no constant values, but display logarithmic increase with increasing retrace velocity. This dependence of f_u on v_r is dictated by changing lifetimes of the adhesion complexes that depend on both intrinsic bond kinetics at zero force and response of the bond kinetics to the applied external forces. The lifetime of bonds at zero force (τ_0) can be estimated from extrapolation of the force-dependent lifetime of the bonds ($\tau(f)$) to zero force, according to Bell's equation (27) and estimation of $\tau(f)$ from the width of the force distribution (20). Fitting Bell's equation to the observed unbinding forces at different retrace velocities (Fig. 4) yields a lifetime of the complex at zero force of $\tau_0 \approx 0.55$ s and a corresponding off rate constant of $k_{off}^0 = \tau_0^{-1} \approx 1.8$ s^{-1} for individual adhesion dimers. The critical bond width of the adhesion dimer follows from this fit of data to be in the range of $l_r \approx 0.59$ nm.

Ca^{2+} Dependency of Adhesive Interaction. Approach-retrace cycles at v_r = 800 nm·s^{-1} and 0.1 s encounter time were performed at different Ca^{2+} concentrations (10 μM to 20 mM). The total area between the force curve and the neutral line was taken as measure for binding activity. Each point of the plot shown in Fig. 5 represents the mean activity of at least 300 retrace cycles. Ca^{2+} dependency of binding activity showed an apparent K_D of 1.15 mM with very steep dependency, indicating a high degree of cooperativity with a Hill coefficient of n_h = 5.04. Maximum level of binding activity seen at Ca^{2+} concentrations >1 mM could be immediately blocked by addition of the monoclonal antibody to mouse VE-cadherin external domain.

Discussion

Cadherin-mediated intercellular adhesion is a basic cellular function involved in a variety of physiological and pathological processes, including embryogenesis, epithelial barrier regulation, and tumor cell metastasis (1, 2). In the present study, we obtained direct proof for the strength and kinetics of adhesive interactions between rod-shaped cis-dimers of the external domains of a classical cadherin (VE-cadherin) investigated by single-molecule recognition force microscopy.

Unit unbinding force (adhesive strength) determined here for a classical cadherin turned out to be relatively weak (35–55 pN at v_r = 200–4,000 nm·s^{-1}) as compared with AFM data of unbinding forces between Ab against albumin and its antigen

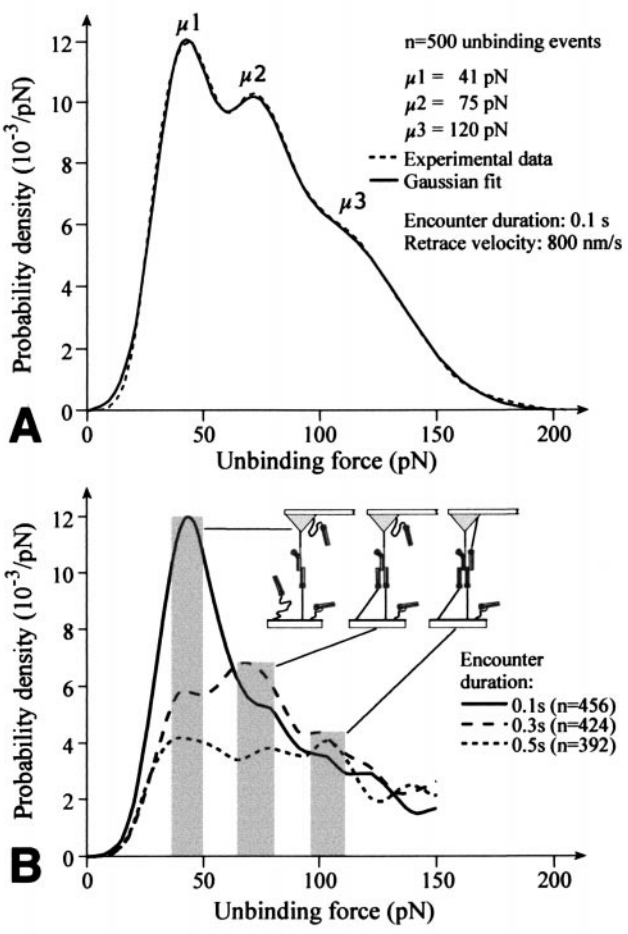

Fig. 3. Frequency distribution of unbinding forces between tip- and plate-attached PEG/VE-cadherin-Fc measured at retrace velocities of 800 nm·s^{-1} and various tip-to-plate encounter intervals. Frequency distribution is expressed as probability density function (n = number of unbinding events). (*A*) Data shown fit to three Gaussian distributions with peak values (μ1–μ3) at about 40, 75, and 120 pN. (*B*) Dependency of the frequency of μ1–μ3 on encounter duration indicates a diffusion-limited reaction underlying multimerization of tip- and plate-bound cadherins. Synchronous dirsuption of independent bonds is highly unlikely (see *Discussion*).

(245 pN at v_r = 200 nm·s^{-1}) (15) as well as between recombinant P-selectin and its ligand PSGL-1 (159 pN at v_r = 2,800 nm·s^{-1}) (28). However, our observations obtained by increasing the encounter time for tip- and plate-bound VE-cadherin-Fc indicate that VE-cadherin is capable of associating into complexes with cumulative binding strength (Fig. 3).

For two main reasons, we believe that these multiples of adhesive strength quanta result from lateral oligomerization and cooperative unbinding of cadherin dimers rather than from formation of independent adhesion dimers disrupting synchronously: (*i*) The spectrum of unbinding lengths (l_u) observed in the study ranged from 30 to 70 nm. This indicates considerable length variations of individual PEG-linked VE-cadherin-Fc dimers. This variation is probably caused by (*a*) variation of the extended chain lengths of PEG (8–40 nm; our observations) and (*b*) by variations of the sites of coupling of the PEG-links to both the VE-cadherin-Fc rod and the curved AFM tip. It is therefore unlikely that synchronous disruption of independent bonds will occur with a significant probability and that this probability depends on the encounter duration. (*ii*) In previous AFM studies with surface-adsorbed P-selectin/PSGL 1 (28) and PEG-linked integrin $\alpha_v\beta_5$/vitronectin

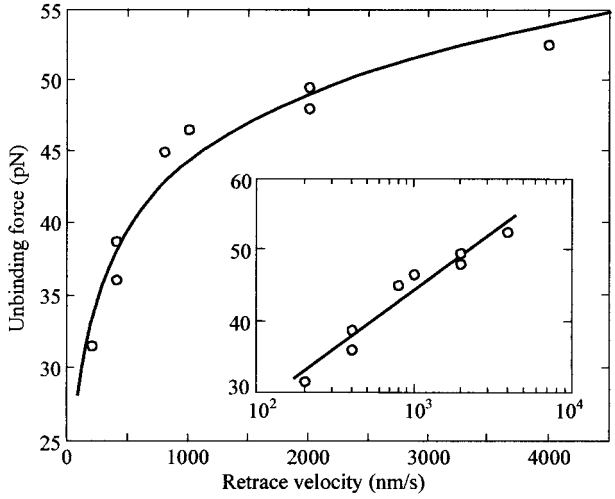

Fig. 4. Dependence of unbinding force of the first peak (corresponding to μ1 in Fig. 3) on retrace velocity plotted in the inset on a logarithmic scale. Each point represents the average value of at least 300 unbinding events measured at a given retrace velocity. The solid line is a numerical fit of the data to modified Bell's expression ($\tau(f_u) = \tau_0 \exp(-l_r f_u/k_BT)$, where τ_0 is the lifetime of unstressed bonds, l_r the unbinding width between adhering cadherins, k_B Boltzman's constant, T is the absolute temperature, and f_u is the unbinding force. The fit yields for $\tau_0 \approx 0.55$ s and for $l_r \approx 0.59$ nm.

(our unpublished data), only simple Gaussian distributions of unbinding forces were observed with no significant higher order disruption events in response to increase of the encounter time. The idea that adhesion dimers may be capable of lateral association into cooperative oligomers was primarily concluded from crystals of subdomain 1 of N-cadherin (5), but such trans-interacting associations were not seen in crystals of subdomains 1–2 of E-cadherin (6, 9).

The lifetime (τ_0) of the trans-interacting VE-cadherin complex at zero force was determined by stepwise increasing v_r from 400

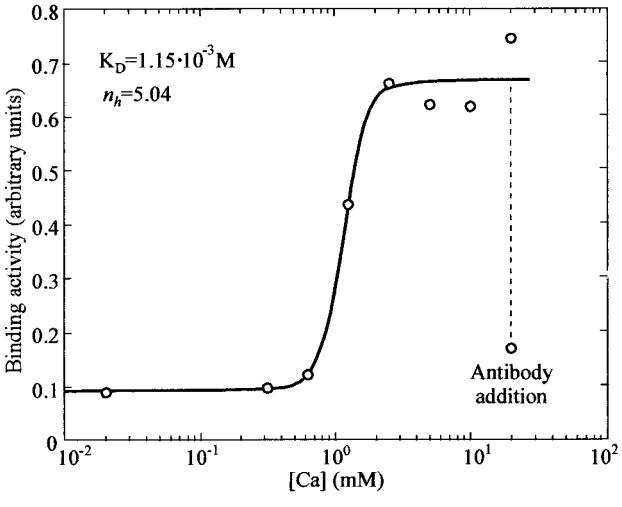

Fig. 5. Ca^{2+}-dependence of binding activity between tip- and plate-attached PEG/VE-cadherin-Fc at various Ca^{2+} concentrations. All measurements were obtained with an individual experimental set-up with stepwise increase of the Ca^{2+} concentration by fluid exchange. Binding activity is defined as area between the force distance curve and the neutral line. Each point is the average of at least 400 force distance cycles. Note pronounced cooperativity with a Hill coefficient of 5.04 and an apparent K_D = 1.15 10^{-3} M. Addition of antibody to VE-cadherin-Fc at 20 mM Ca^{2+} caused immediate and almost complete inhibition of binding.

to 4,000 nm·s^{-1}, yielding $\tau_0 \approx 0.55$ s, which corresponds to a dissociation rate constant of $k_{off} = \tau_0^{-1} \approx 1.8$ s^{-1}. This value is in the range of the unstressed dissociation rate determined for bonds between various selectins and their ligands: 1–1.4 s^{-1} for P-selectin, 0.7 s^{-1} for E-selectin, and 7 s^{-1} for L-selectin (29–31). The calculated on rate constant (k_{on}) for unforced equilibrium trans-interaction between VE-cadherin strand dimers (calculated from exponential dependency of the probability of recognition events with half maximal value at $t_{0.5} = 0{,}08$ s and effective concentration of tip-bound molecules in the boundaries of 10^{-3}–10^{-5} M; data not shown) appears to be one to two orders of magnitude lower ($k_{on} \approx 10^3$–10^4 M^{-1}·s^{-1}) than the k_{on} values determined for bonds between P-selectin and PSGL-1 ($\approx 10^5$–10^6 M^{-1}·s^{-1}) (28, 31). The resulting affinity between trans-interacting VE-cadherins ($K_D \approx 10^{-3}$–10^{-5} M) is similar to that between lymphocyte CD2 and CD48 adhesion molecules ($K_D \approx 10^{-4}$ M) (32) but significantly lower than that of P-selectin-mediated adhesion ($K_D \approx 10^{-7}$–10^{-8} M). These affinity differences between selectin- and cadherin-mediated adhesion have important biological implications. Binding between leukocytes and endothelial cells must occur under the hydrodynamic loads of blood flow that require a high k_{on} to increase probability of bond formation. Cadherins, on the other hand, mediate adhesion between resting cells. Thus, mechanical stress on the junctions is less intense and high binding affinities may not be required to establish and maintain intercellular adhesion. However, low-affinity binding by means of cadherins may be a prerequisite for dynamic cell behavior to occur, such as remodeling of cell shape, or down- and up-regulation of the barrier properties of epithelial/endothelial layers (1–3). Likwise, remodeling of actin filament meshworks appears to be also driven by low-affinity interactions (33).

A likely mechanism by which cadherin-mediated adhesion might be regulated would be by immobilization of the cadherins by tethering their cytoplasmic domains to the actin filament cytoskeleton. This would significantly restrain lateral mobility in the plane of the lipid bilayer (as shown by single particle tracking for E-cadherin; ref. 34), and, significantly, increase the probability of a given cadherin strand dimer to rebind (trans-interact) after dissociation rather than to move apart by lateral diffusion. In addition, cytoskeletal tethering would strongly favor both assembly and lifetime of clustered higher order complexes. Any signaling mechanisms changing cytoskeletal tethering of cadherins, e.g., by phosphorylation of catenin adaptor molecules (3) or by modulation of the state of actin polymerization, would have an important impact on the lateral mobility (translational entropy) of cadherins, and thus, on the number of adhesive bonds. This view of a cytoskeletal cooperativity (which would be particularly effective at weak external binding affinity of cadherins) is supported by observations showing that cadherin-mediated cellular adhesion is strongly dependent on catenin/cytoskeleton binding to the cytoplasmic domain (35–37) and, furthermore, is supported by crosslinking experiments of the cytoplasmic domain of C-cadherin that resulted in significant increase of the strength of cellular adhesion (38).

Determination of Ca^{2+}-dependency of recognition events between tip- and plate-bound VE-cadherin-Fc revealed surprisingly high K_D (1.15 mM Ca^{2+}), which is close to the free extracellular Ca^{2+} concentration in the body (1.2 mM) (39). This and the extremely steep Ca^{2+}-activity relation with a Hill coefficient of about 5 opens the interesting possibility that a local drop of free extracellular Ca^{2+} in the narrow intercellular clefts (i.e., caused by opening of store-operated Ca^{2+}-channels; refs. 40 and 41) might weaken intercellular adhesion and facilitate cellular remodeling and inflammatory dissociation of endothelial cells. However, short-term changes of endothelial permeability (as induced by various vasoactive substances; refs. 42 and 43) are probably not regulated by cadherin-based adhesion, because Ca^{2+} concentrations close to zero do not acutely decrease endothelial barrier properties despite complete loss of VE-cadherin from junctions (42, 44, 45). Tight junctions and additional Ca^{2+}-independent adhesion molecules may be capable of compensating loss of VE-cadherin for a certain time interval (45). Excitation-induced localized depletion of extracellular Ca^{2+} from intercellular space has been recently reported for synaptic junctions in the central nervous system, where regulation of cadherins by changes of extracellular Ca^{2+} concentrations have been suggested to be involved in synaptic remodelling associated with long term potentiation (46). Loss of trans-interaction between VE-cadherin at Ca^{2+} concentration below 0.5 mM corresponds to collapse of the elongated VE-cadherin-Fc in low Ca^{2+} and dissociation into monomeric strands (Fig. 1*B*). Similar observations were obtained with recombinant E-cadherin external domain that require Ca^{2+} concentrations of 45–150 μM for elongation of monomeres (47) and Ca^{2+} concentrations above 0.5 mM ($K_D \approx 2$ mM) to saturate remaining low affinity Ca^{2+}-binding sites that appear to be critical for both cis-dimerization and trans-interaction (48).

This study was supported by a grant from the Deutsche Forschungsgemeinschaft (SFB 487, B5).

1. Gumbiner, G. M. (1996) *Cell* **84,** 345–357.
2. Takeichi, M. (1995) *Curr. Opin. Cell Biol.* **7,** 619–627.
3. Lampugnani, M. G. & Dejana, E. (1997) *Curr. Opin. Cell Biol.* **9,** 674–682.
4. Chothia, C. & Jones, E. Y. (1997) *Annu. Rev. Biochem.* **66,** 823–862.
5. Shapiro, L., Fannon, A. M., Kwong, P. D., Thomposn, A., Lehmann, M. S., Grubel, G., Legrand, J. F., Als-Nielsen, J., Colman, D. R. & Hendrickson, W. A. (1995) *Nature (London)* **374,** 327–337.
6. Nagar, B., Overduin, M., Ikura, M. & Rini, J. M. (1996) *Nature (London)* **380,** 360–364.
7. Koch, A. W., Bozic, D., Pertz, O. & Engel, J. (1999) *Curr. Opin. Cell Biol.* **9,** 275–281.
8. Brieher, W. M., Yap, A. S. & Gumbiner, B. M. (1996) *J. Cell Biol.* **135,** 487–496.
9. Pertz, O., Bozic, D., Koch, A. W., Fauser, F., Brancaccio, A. & Engel, J. (1999) *EMBO J.* **18,** 1738–1747.
10. Binnig, G., Quate, C. F. & Gerber, C. (1986) *Phys. Rev. Lett.* **56,** 930–933.
11. Florin, E. L., Moy, V. T. & Gaub, H. E. (1994) *Science* **264,** 415–417.
12. Lee, G. U., Kidwell, D. A. & Colton, R. J. (1994) *Langmuir* **10,** 354–357.
13. Müller, D. J., Schabert, F. A., Büldt, G. & Engel, A. (1995) *Biophys. J.* **68,** 1681–1686.
14. Shao, Z. & Yang, J. (1995) *Q. Rev. Biophys.* **28,** 195–251.
15. Hinterdorfer, P., Baumgartner, W., Gruber, H. J., Schilcher, K. & Schindler, H. (1996) *Proc. Natl. Acad. Sci. USA* **93,** 3477–3481.
16. Gotsch, U., Borges, E., Bosse, R., Böggemeyer, E., Simon, M., Mossmann, H. & Vestweber, D. (1997) *J. Cell Sci.* **110,** 538–588.
17. Han, W., Lindsay, S. M. & Jing, T. (1996) *Appl. Phys. Lett.* **69,** 1–3.
18. Han, W., Lindsay, S. M., Dlakic, M. & Harrington, R. E. (1997) *Nature (London)* **386,** 563.
19. Haselgrübler, T., Amerstorfer, A., Schindler, H. & Gruber, H. J. (1995) *Bioconjugate Chem.* **6,** 242–248.
20. Hinterdorfer, P., Schilcher, K., Baumgartner, W., Gruber, H. J. & Schindler, H. (1998) *Nanobiology* **4,** 177–188.
21. Willemsen, O. H., Snel, M. M. E., van der Werf, K. O., de Grooth, B. G., Greve, J., Hinterdorfer, P., Gruber, H. J., Schindler, H., VanKooyk, Y. & Figdor, C. G. (1998) *Biophys. J.* **75,** 2220–2228.
22. Hutter, J. L. & Bechhoefer, J. (1993) *Rev. Sci. Instrum.* **64,** 1868–1873.
23. Baumgartner, W., Hinterdorfer, P. & Schindler, H. (2000) *Ultramicroscopy* **82,** 85–95.
24. Evans, E. & Ritchie, K. (1997) *Biophys. J.* **72,** 1541–1555.
25. Grubmüller, H., Heymann, B. & Tavan, B. (1996) *Science* **271,** 997–999.
26. Rief, M., Gautel, M., Oesterhelt, F., Fernandesz, J. M. & Gaub, H. E. (1997) *Science* **276,** 1109–1112.
27. Bell, G. I. (1978) *Science* **200,** 618–627.
28. Fritz, J., Katopodis, A. G., Kolbinger, F. & Anselmetti, D. (1998) *Proc. Natl. Acad. Sci. USA* **95,** 12283–12288.
29. Alon, R., Hammer, D. A. & Springer, T. A. (1995) *Nature (London)* **374,** 539–542.
30. Alon, R., Chen, S. Q., Puri, K. D., Finger, E. B. & Springer, T. A. (1997) *J. Cell Biol.* **138,** 1169–1180.

31. Mehta, P., Cummings, R. D. & McEver, R. P. (1998) *J. Biol. Chem.* **273,** 32506–32513.
32. Pierres, A., Benoliel, A. M., Bongrand, P. & van der Merwe, P. A. (1996) *Proc. Natl. Acad. Sci. USA* **93,** 15114–15118.
33. Sato, M., Schwarz, W. H. & Pollard T. D. (1987) *Nature (London)* **325,** 828, 830.
34. Sako, Y., Nagafuchi, A., Tsukita, S., Takeichi, M. & Kusumi, A. (1998) *J. Cell Biol.* **140,** 1227–1240.
35. Chen, H., Paradies, N. E., Fedor-Chaiken, M. & Brackenbury, R. (1997) *J. Cell Sci.* **110,** 345–356.
36. Schnittler, H., Püschel, B. & Drenckhahn, D. (1997) *Am. J. Physiol.* **273,** 2396–2405.
37. Ozawa, M. & Kemler, R. (1998) *J. Cell Biol.* **142,** 1605–1613.
38. Yap, A. S., Brieher, W. M., Pruschy, M. & Gumbiner, B. M. (1997) *Curr. Biol.* **7,** 308–315.
39. Parfitt, A. M. (1993) in *Handbook of Experimental Pharmacology* (Springer, Heidelberg), Vol. 107, pp. 1–65.
40. Groschner, K., Hingel, S., Lintschinger, B., Balzer, M., Romanin, C., Zhu, X. & Schreibmayer, W. (1998) *FEBS Lett.* **437,** 101–106.
41. Moore, T. M., Brough, G. H., Babal, P., Kelly, J. J., Li, M. & Stevens, T. (1998) *Am. J. Physiol.* **275,** L574–L582.
42. Michel, C. C. & Curry, F. E. (1999) *Physiol. Rev.* **79,** 703–761.
43. Drenckhahn, D. & Ness, W. (1997) in *Vascular Endothelium: Physiology, Pathology, and Therapeutic Opportunities*, eds. Born, G. V. R. & Schwartz, C. J. (New Horizon Series 3**,** Schattauer, Stuttgart), pp. 1–25.
44. Suttorp, N., Fuchs, T., Seeger, W., Wilke, A. & Drenckhahn, D. (1989) *Lab. Invest.* **61,** 183–191.
45. Schnittler H., Wilke, A., Gress, T., Suttorp, N. & Drenckhahn, D. (1990) *J. Physiol.* **431,** 379–401.
46. Tang, L., Hung, C. P. & Schuman, E. M. (1998) *Neuron* **20,** 1165–1175.
47. Pokutta, S., Herrenknecht, K., Kemler, R. & Engel, J. (1994) *Eur. J. Biochem.* **223,** 1019–1026.
48. Pertz, O., Bozic, D., Koch, A. W., Fauser, C., Brancaccio, A. & Engel, J. (1999) *EMBO J.* **18,** 1738–1747.